Journal of Integrative Neuroscience, Vol. 5, No. 4 (2006) 561–593
© Imperial College Press

Imperial College Press
www.icpress.co.uk

Research Report

GENERATION OF THE RECEPTIVE FIELDS OF SUBPIAL CELLS IN TURTLE VISUAL CORTEX

WENXUE WANG[*,‡], SEAN LUO[†,§], BIJOY K. GHOSH[*,¶]
and PHILIP S. ULINSKI[†,**]

[*]*Department of Electrical and Systems Engineering*
Washington University
Campus Box 1127, Bryan Hall 201
One Brookings Dr.
Saint Louis, MO 63130

[†]*Committee on Computational Neuroscience*
The University of Chicago
1025 E. 57th Street
Chicago, IL 60637
[‡]*ww1@ese.wustl.edu*
[§]*xsl2101@columbia.edu*
[¶]*ghosh@netra.wustl.edu*
[**]*pulinski@uchicago.edu*

Received 15 September 2006
Accepted 14 November 2006

The visual cortex of turtles contains cells with at least two different receptive field properties. Superficial units are located immediately below the pial surface. They fire in response to moving bars located anywhere in binocular visual space and to two spots of light presented with different spatiotemporal separations. Their location in the cortex suggests that superficial units correspond to a distinct class of inhibitory interneurons, the subpial cells, that are embedded in geniculocortical axons as they cross the visual cortex of turtles. This study used a detailed compartmental model of a subpial cell and a large-scale model of visual cortex to examine the cellular mechanisms that underlie the formation of superficial units on the assumption that they are subpial cells. Simulations with the detailed model indicated that the biophysical properties of subpial cells allow them to respond strongly to activation by geniculate inputs, but the presence of dendritic beads on the subpial cells decreases their sensitivity and allows them to integrate the inputs from many geniculate afferents. Simulations with the large-scale model indicated that the responses of subpial cells to simulated visual stimuli consist of two phases. A fast phase is mediated by direct geniculate inputs. A slow phase is mediated by recurrent excitation from pyramidal cells.

[‡]Corresponding author.

It appears that subpial cells play a major role in controlling the information content of visual responses.

Keywords: Inhibitory interneurons; dendritic beads.

1. Introduction

F 35. 21 D $800\,\mu$ $1000\,\mu$ $15°/$ $8°/$. D , t. t $t = 50$ $t = 200$ $t = 500$ $t = 1000$ 35. $200\,\mu$ $300\,\mu$ 21. . . t. $t = 10$ 100 $t = 100$ 700 . (6, 7, 9) . H D 2 7. 1 6. G D 9. 1, 6, 34.

[illegible] 2, 28, [illegible] GABA- [illegible] A [illegible] 6 [illegible] 13, 22. [illegible] 70% [illegible] 6. [illegible] 6, 16, 19. [illegible] F [illegible] . F [illegible]

[illegible]

2. Methods

2.1. *Anatomy and physiology*

[illegible] *Neurobiotin* [illegible] C [illegible] *et al.* 6. [illegible] 1 [illegible] A [illegible] 2A [illegible] (A [illegible]). [illegible] *Neurobiotin*- [illegible]. A [illegible]

0.1 μ 510 ( ).

3-12-99 12 C *et al.* 7 134 μ D. 66 μ . 26 μ 120 μ . 3-12-99 113 μ 206 μ . 60 μ 260 μ . 205 μ 520 μ . 3-12-99 A F F 1. . 3-12-99 138 73.2% , 84 17.9% . 139 56.2% , 85 12.3% . 3-2-99

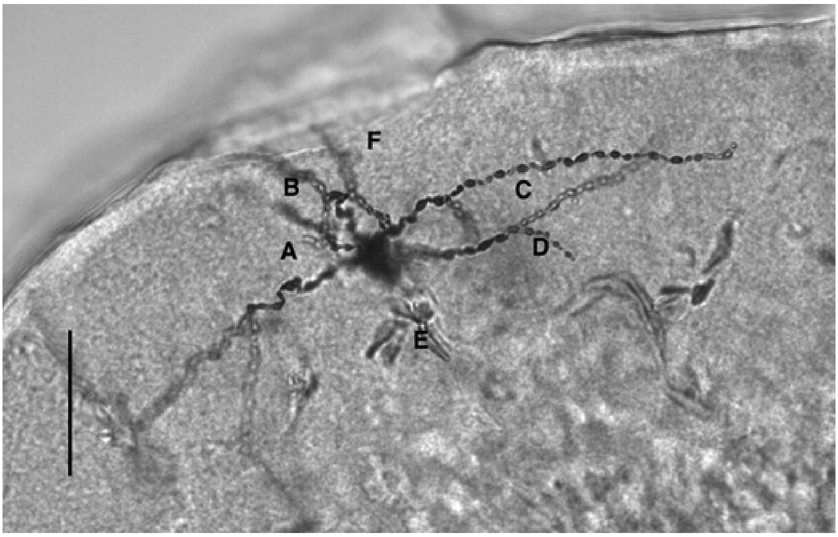

Fig. 1. Morphology of cell 3-12-99. This is a confocal micrograph of cell 3-12-99. The primary dendrites are labeled A through F. The pial surface is the arc across the top of the figure. Pyramidal cells in layer 2 of the cortex are visible at the lower right edge of the image. The lateral edge of the cortex is to the right. Thus, geniculate afferents enter the image from the left and proceed in an arc across the image. The vertical scale represents 50 μm.

8.9% [illegible] 5419.3 μ ^{2}. [illegible] 31.5% [illegible] 5990.1 μ ^{2}. [illegible] 3-12-99 [illegible]. [illegible] 3-12-99 [illegible] 1.3 G [illegible] $R_m = 70$ [illegible] ^{2}. [illegible] 12 [illegible] 0.179 G [illegible] 2.0 G [illegible]. [illegible] 3-12-99 [illegible] $\tau_0 = 31.5$ [illegible] $\tau_1 = 1.2$ [illegible] 11 [illegible] 21.6 [illegible] 89.4 [illegible] 1.4 [illegible] 2.3 [illegible] 0.5 [illegible] 2.1. F [illegible] 2A [illegible] +0.02 [illegible] +0.03 A [illegible]. [illegible] F [illegible] 2B [illegible] +0.03 A [illegible]. [illegible] F [illegible] 2C, [illegible] H [illegible] (F [illegible] 2A, −0.07 A).

2.2. *Full compartmental model*

E [illegible] 138 [illegible] 84 [illegible] 3-12-99 [illegible]. F [illegible] 3A [illegible]. A [illegible] (F [illegible] 3B).

E [illegible] (B [illegible] B [illegible] 5):

$$\frac{dV_i(t)}{dt} = -\frac{1}{C_i}\left[\frac{(V_i(t) - E_r)}{R_i} + \sum_j \frac{V_i(t) - V_j(t)}{R_{ij}} + \sum_{ion} g_k(V_i(t) - E_k) + \sum_{syn} g_k(V_i(t) - E_k) + I_{stim}(t)\right] \quad (2.1)$$

[illegible] $V_i(t)$ [illegible] i [illegible], C_i [illegible]

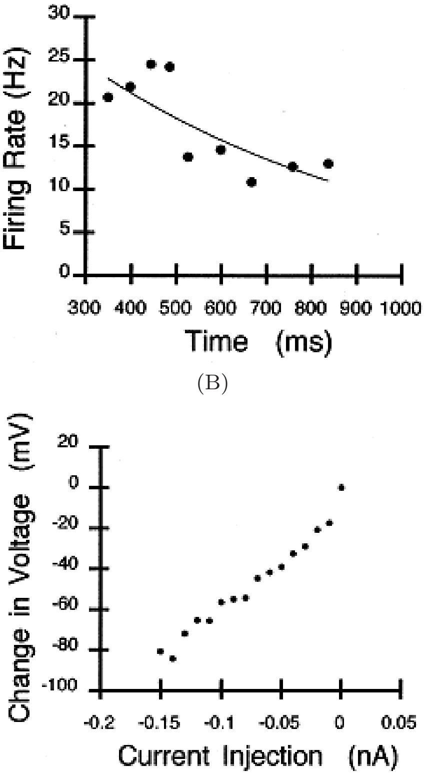

(B)

(C)

(A)

Fig. 2. Responses of cell 3-12-99 to intrasomatic current pulses. (A) Responses of the cell 3-12-99 to 1 s current pulses with amplitudes of +0.01 nA, +0.02 nA, +0.03 nA and −0.07 nA. (B) Firing rate adaptation curve. The instantaneous firing rate of cell 3-12-99 is plotted as a function of time after the onset of the current pulse, which took place at 300 ms. (C) Voltage-current plot for cell 3-

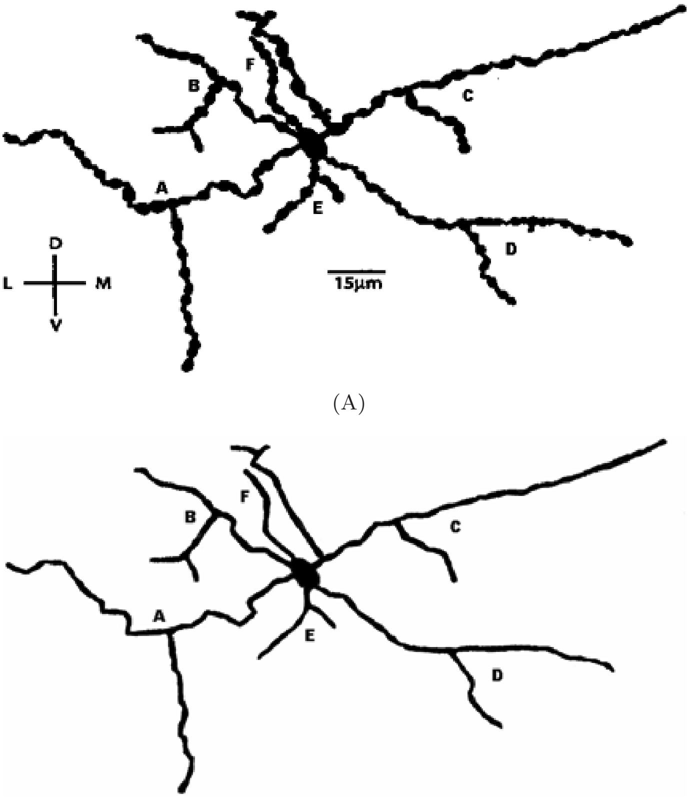

(A)

(B)

Fig. 3. Structure of compartmental models. This figure illustrates the morphological structure used for full and reduced compartmental models used in this study. (A) Structure of the full compartmental model. The soma and each varicosity and intervaricose segment are included. The primary dendrites are labeled A through F. Compare this drawing to the confocal image in Fig. 1. (B) Structure of the reduced compartmental model. Individual compartments are numbered.

[illegible] F [illegible] 4B [illegible] ([illegible] , [illegible]) [illegible] ([illegible] , [illegible]) [illegible] −0.01 A [illegible] , [illegible] . [illegible] - [illegible] - [illegible] .

2.3. *Reduced compartmental model*

A [illegible] 3-12-99 (F [illegible] 5) [illegible] 223 [illegible] 29 [illegible] *et al.* 33. [illegible] , [illegible] F [illegible] , [illegible]

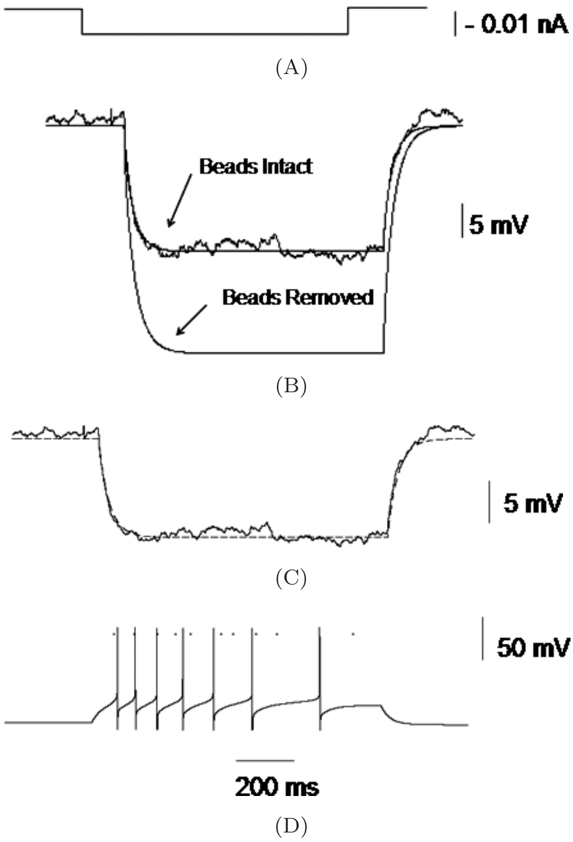

Fig. 4. Biophysical characteristics of compartmental models. This figure illustrates the responses of cell 3-12-99 and the full and reduced compartmental models to intrasomatic current pulses. (A) A -0.01 nA, 1 s current pulse. (B) The response of cell 3-12-99 to the -0.01 nA current pulse superimposed on the response of the passive model with beads intact in the upper two traces. The lower trace shows the response of the passive model with beads removed. (C) The response of cell 3-12-99 to a -0.01 nA current pulse superimposed on the response of the reduced compartmental model. (D) The response of the reduced compartmental model to a $+0.02$ nA current pulse. The occurrence times of spikes in cell 3-12-99 to a $+0.02$ nA current pulse are shown by dots.

[illegible] $l_i' = l_i\sqrt{d_r/d_i}$ [illegible] l_i [illegible] i [illegible], d_i [illegible] d_r [illegible] l_i' [illegible]. [illegible] $d_c = (\sum_{i=1}^{n} d_i^{3/2})^{2/3}$ [illegible] d_c [illegible], n [illegible] d_i [illegible] i [illegible]

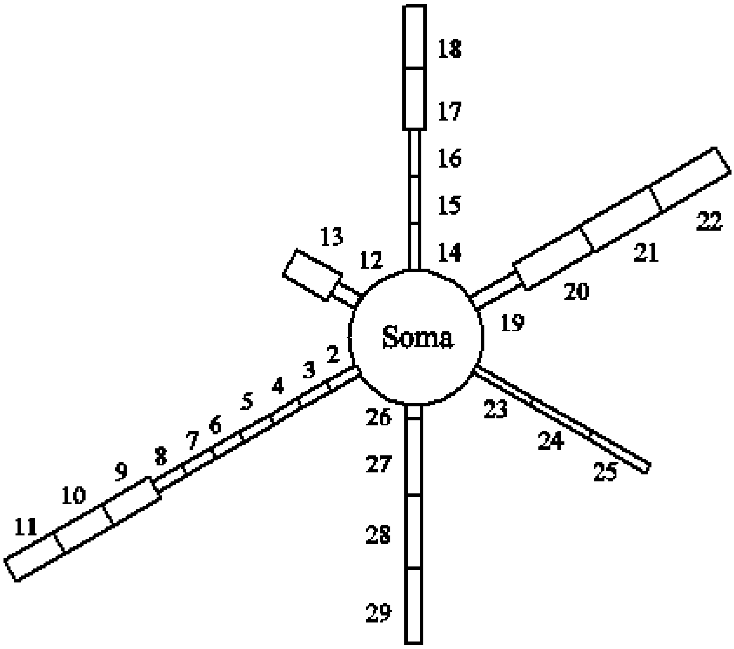
18
17
16
15
14
13
12
Soma
2
3
4
5
6
7
8
9
10
11
19
20
21
22
23
24
25
26
27
28
29

Fig. 5. Structure of the reduced compartmental model. Each soma and dendritic compartment in the reduced model is numbered.

$l_c = l_s\sqrt{d_c/d_r}$ [illegible] $l_s = \left(\sum_{i=1}^{n} l'_i\right)/n$. [illegible], [illegible] F [illegible] 3B [illegible] 2 [illegible] 29. [illegible] 1. F [illegible] 4C [illegible] -0.01 A [illegible]. [illegible] $R_m = 34.7$ [illegible] ^{2}. [illegible] $C_m = 0.4\,\mu\mathrm{F}/$ [illegible] ^{2}. [illegible] $R_a = 285.6$ [illegible]. [illegible] $V_r = -74.0$ [illegible].

2.4. *Active conductances*

[illegible] $(I_{\mathrm{Na}}(V,t))$ [illegible] $(I_{\mathrm{DR}}(V,t))$ [illegible] H [illegible] -H [illegible]

Table 1. Dimensions of compartments in reduced subpial cell model.

Compartment	Diameter	Length	E_length	Connections
Soma	9.5 μm			
Dend2	0.13 μm	37 μm	0.19	To soma
Dend3	0.13 μm	37 μm	0.19	To dend2
Dend4	0.13 μm	37 μm	0.19	To dend3
Dend5	0.13 μm	37 μm	0.19	To dend4
Dend6	0.13 μm	37 μm	0.19	To dend5
Dend7	0.13 μm	37 μm	0.19	To dend6
Dend8	0.13 μm	37 μm	0.19	To dend7
Dend9	0.31 μm	57 μm	0.19	To dend8
Dend10	0.31 μm	57 μm	0.19	To dend9
Dend11	0.31 μm	57 μm	0.19	To dend10
Dend12	1.46 μm	13 μm	0.02	To soma
Dend13	1.65 μm	54 μm	0.08	To dend12
Dend14	0.57 μm	57 μm	0.14	To soma
Dend15	0.57 μm	57 μm	0.14	To dend14
Dend16	0.57 μm	57 μm	0.14	To dend15
Dend17	0.69 μm	70 μm	0.15	To dend16
Dend18	0.69 μm	70 μm	0.15	To dend17
Dend19	0.46 μm	52 μm	0.14	To soma
Dend20	1.15 μm	95 μm	0.16	To dend19
Dend21	1.15 μm	95 μm	0.16	To dend20
Dend22	1.15 μm	95 μm	0.16	To dend21
Dend23	0.36 μm	59 μm	0.18	To soma
Dend24	0.36 μm	59 μm	0.18	To dend23
Dend25	0.36 μm	59 μm	0.18	To dend24
Dend26	0.95 μm	6 μm	0.01	To soma
Dend27	0.95 μm	89 μm	0.17	To dend26
Dend28	0.95 μm	89 μm	0.17	To dend27
Dend29	0.95 μm	89 μm	0.1667	To dend28

([illegible] *et al.*, [illegible] 24), [illegible] CA3 [illegible] ($I_{\mathrm{Ca}^{2+}}(V,t)$) [illegible] AH [illegible] (I_{AHP}([illegible]C[illegible]$^{2+}$, t), [illegible] AH [illegible], C[illegible]$^{2+}$. [illegible]. F[illegible] 4D [illegible] +0.02 [illegible] A [illegible].

[illegible]. H [illegible] *et al.* 24. [illegible]

[illegible]: $\bar{g}_{\mathrm{Na}^+} = 370$ [illegible]^2; $\bar{g}_{\mathrm{K}^+} = 250$ [illegible]^2; $\bar{g}_{\mathrm{K}^+_{\mathrm{AHP}}} = 0.02$ [illegible]^2; $\bar{g}_{\mathrm{Ca}^{2+}} = 2.3$ [illegible]^2. [illegible]

[illegible]: $\bar{g}_{\mathrm{Na}^+} = 3256$ [illegible]^2; $\bar{g}_{\mathrm{K}^+} = 2200$ [illegible]^2; $\bar{g}_{\mathrm{K}^+_{\mathrm{AHP}}} = 0.15$ [illegible]^2; $\bar{g}_{\mathrm{Ca}^{2+}} = 3.7$ [illegible]^2.

2.5. *Synapses*

B [illegible] G [illegible] α- [illegible] -3- [illegible] 5- [illegible] -4- [illegible] (A A) [illegible] 3, 17. [illegible] A A [illegible] A A [illegible] A A [illegible] +2.9 [illegible] 3 [illegible] 0 [illegible] A A [illegible]. F [illegible], [illegible] τ_1 [illegible] τ_2, [illegible] (E [illegible]) [illegible] (C [illegible], [illegible]). [illegible] E [illegible] E [illegible]. [illegible] E [illegible]. [illegible] E [illegible], [illegible]. [illegible] $\bar{g}_{\mathrm{AMPA}} = 40$ [illegible], $\tau_1 = 1.5$ [illegible] $\tau_2 = 0.5$

G [illegible] 22 [illegible] 6, [illegible] *en passant* 22. [illegible], [illegible] 39 [illegible]. [illegible], 39 [illegible]. A [illegible]

[illegible] 50 μ [illegible]. A [illegible], 0.18 μ [illegible] 7. G [illegible] 4. D [illegible] B [illegible] 4 [illegible] 0, 11, 107, 235, 246 [illegible] 252 [illegible] 20 [illegible]

2.6. *Large-scale model*

[illegible] (F [illegible] 6). E [illegible] 12 16 [illegible] G [illegible] B [illegible] E [illegible] H [illegible] -H [illegible] G [illegible]. [illegible] 1 [illegible] 201 [illegible]. G [illegible]

[illegible] *et al.* 23 [illegible]. [illegible] 44 [illegible] 3-12-99, [illegible]. [illegible] 1 [illegible] 44. [illegible] A A A [illegible] 25 μ . [illegible], 16 [illegible] 1 [illegible], 2 [illegible] 2 [illegible] 2 [illegible] 3 [illegible] 1 [illegible] 4 [illegible]

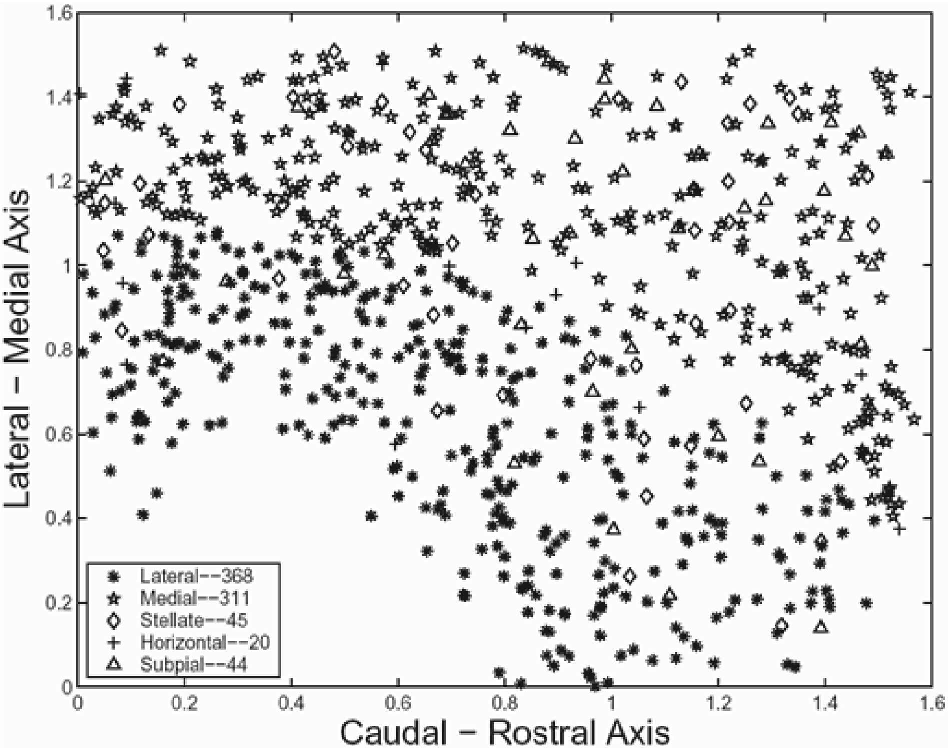

Fig. 6. Spatial distribution of model cells in the large-scale model. This figure shows the spatial distribution of lateral pyramidal, medial pyramidal, stellate, horizontal and subpial cells on an x, y coordinate system. The numbers in the inset at the lower left indicate the number of cells of each type in the model. The dimensions of the grid are 1.6 mm on each side. Rostral is to the left. The lower edge of the coordinate system represents the lateral edge of the visual cortex.

[illegible] A[illegible] A[illegible]. [illegible] $\bar{g}_{\mathrm{AMPA}} = 5.0$ [illegible] $\tau_1 = 3.0$ [illegible] $\tau_2 = 0.3$ [illegible] *et al.* 24. A[illegible] A[illegible] A-[illegible] DA-[illegible] 6 [illegible] 250 μ [illegible] A[illegible] A-[illegible] DA-[illegible] 16 [illegible] $\bar{g}_{\mathrm{AMPA}} = \bar{g}_{\mathrm{NMDA}} = 5.0$ [illegible] $\tau_1 = 3.0$ [illegible] $\tau_2 = 0.3$ [illegible] A[illegible]BA[illegible] $\tau_1 = 80.0$ [illegible] $\tau_2 = 0.67$ [illegible] DA[illegible] GABA[illegible] 4 [illegible]

[illegible] 2 [illegible] 350 μ [illegible]. [illegible] GABA$_A$ [illegible] GABA$_B$ [illegible] GABA [illegible] $\bar{g}_{\text{GABA}} = 5.0$ [illegible] 24 [illegible] 350 μ [illegible]. [illegible] GABA [illegible] GABA$_A$ [illegible] GABA$_B$ [illegible] GABA [illegible] GABA [illegible] $\bar{g}_{\text{GABA}} = 3.5$ [illegible] $\tau_1 = 1.7$ [illegible] $\tau_2 = 1.7$ [illegible] GABA$_A$ [illegible] $\tau_1 = 500.0$ [illegible] $\tau_2 = 500.0$ [illegible] GABA$_B$ [illegible] GABA [illegible] *et al.* [illegible] 24 [illegible].

2.7. *Simulations*

[illegible] *Genesis* [illegible] 5 [illegible] D [illegible] 1 G [illegible] A [illegible] 1 GH [illegible]. [illegible] 2 [illegible] D [illegible] 150 [illegible] 201 [illegible] 150 [illegible] 20 [illegible] 1500 [illegible]

3. Results

3.1. *Integration of geniculate inputs by subpial cells*

[illegible].

[illegible] E [illegible]

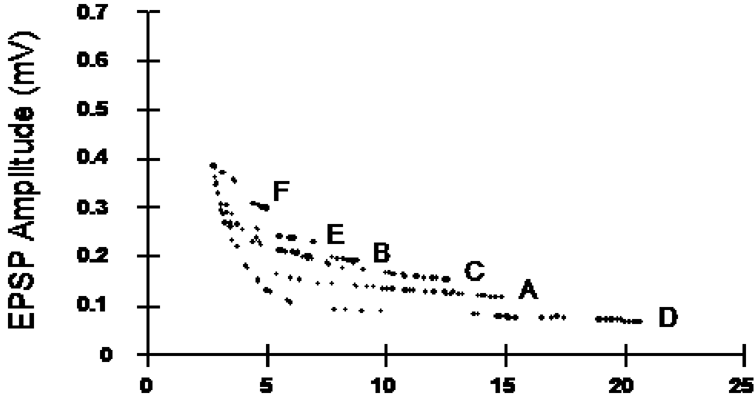

(A) Beads Intact

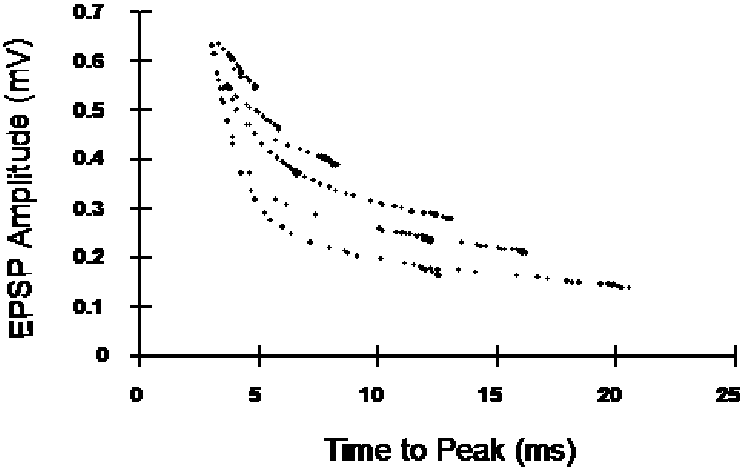

(B) Beads Removed

Fig. 7. Shape-index plots for passive full compartment models. These plots show the amplitudes of EPSPs generated by activation of single synapses in each soma and dendritic compartment of the two passive full compartment models and recorded in the soma compartment of the respective model. Amplitudes of EPSPs are plotted on the vertical axes. Times-to-peak of the EPSPs are plotted on the horizontal axes. EPSPs generated in each dendrite produce an arc of points in the shape index plots. The arcs resulting from primary dendrites A through F of cell 3-12-99 are indicated on the upper plot. (A) The shape index plot for the full compartment model with beads intact. (B) The shape index plot for the full compartment model with beads removed.

[illegible] (F[illegible] 7A). [illegible] E [illegible] 25% [illegible] E [illegible] E [illegible] . F[illegible] 7B [illegible] E [illegible] E [illegible]

[illegible] F[illegible] 4B. [illegible] 1.6 [illegible] 12.3 G[illegible] 1.6 [illegible] A [illegible] $\tau_0 = 37.0$ [illegible] $\tau_1 = 1.1$ [illegible] E [illegible]

[illegible] 16 μ [illegible] 22. [illegible] 0.18 μ [illegible] /μ [illegible] 88 μ [illegible] 1.1 [illegible] 200 μ [illegible] 3-12-99. A [illegible] E [illegible] 36 [illegible] 39 [illegible] A [illegible] E [illegible] E [illegible] ([illegible]) [illegible] C [illegible] 39. A [illegible] 37 [illegible] E [illegible] A [illegible] 138 [illegible] (F[illegible] 8A). B[illegible] 12 [illegible] (F[illegible] 8B). A [illegible] 138 [illegible] (F[illegible] 8B). [illegible] E [illegible]

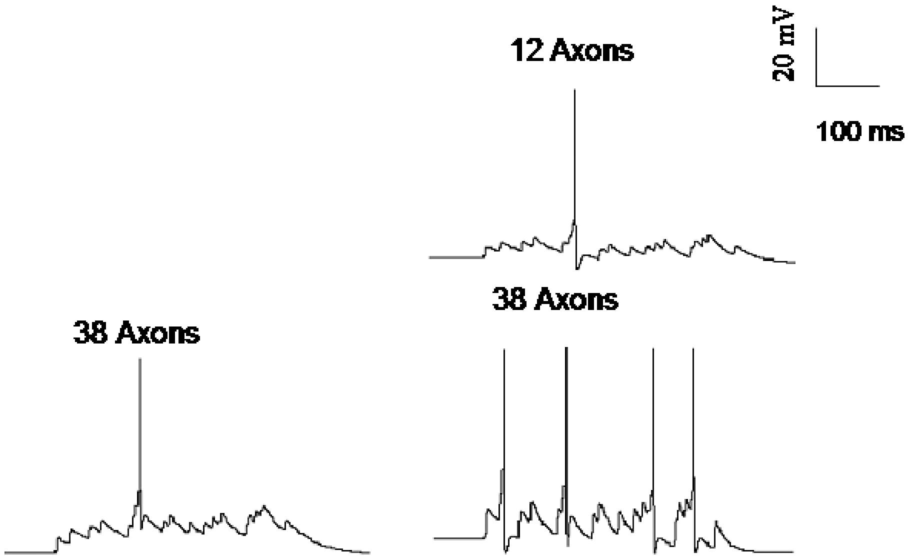

(A) With Beads (B) Without Beads

Fig. 8. Responses of model cells with active conductances to the asynchronous activation of geniculate afferents. (A) An action potential produced in the full compartmental model with active conductances by activation of 38 geniculate axons when beads are intact. Activation of fewer than 38 axons did not produce an action potential. (B) Activation of 12 axons produced a single action potential in the full compartmental model when beads are removed. Activation of 38 geniculate afferents produced multiple action potentials.

3.2. *Responses of subpial cells to simulated diffuse light flashes*

F[illegible] 9A [illegible] 20 [illegible] 180 [illegible] 330 [illegible] 950 [illegible] F[illegible] 10A, [illegible] 44 [illegible] 21 [illegible] 44 [illegible] 200 [illegible] 22 [illegible] 200 [illegible] 1000 [illegible]

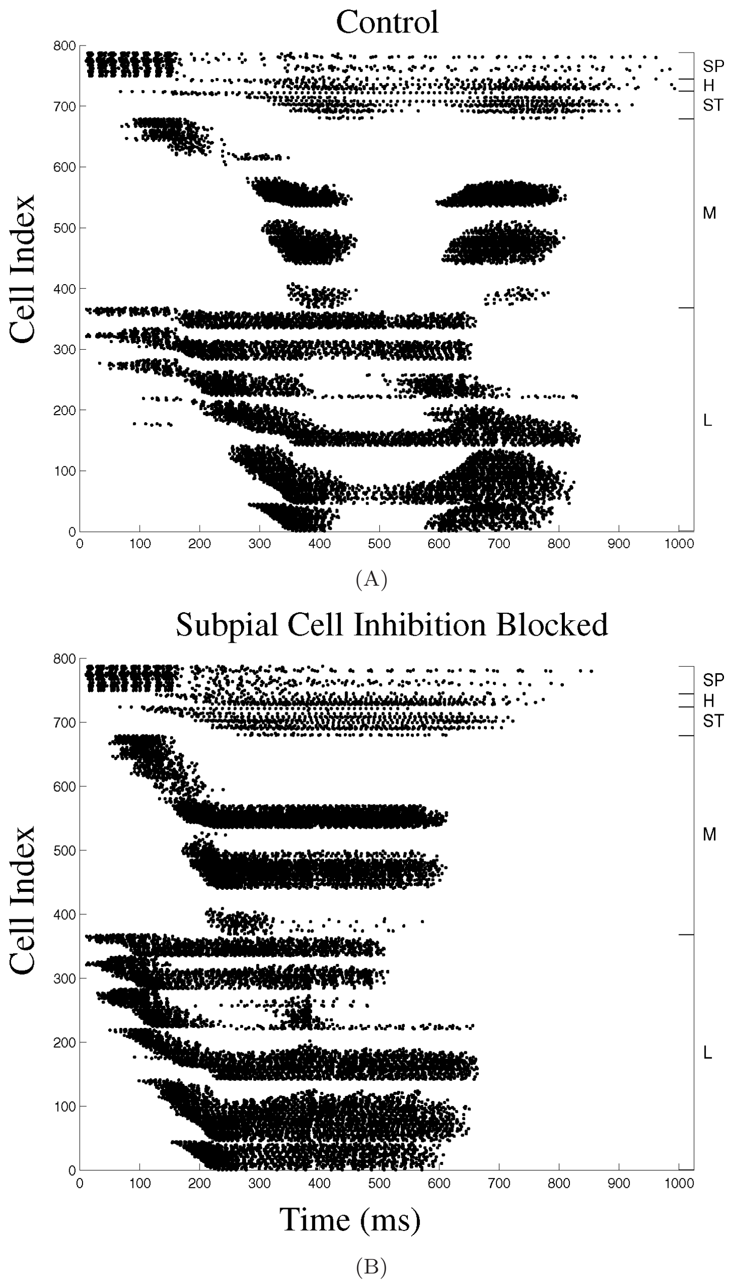

Fig. 9. Responses of subpial cells to simulated diffuse light flashes. Responses of the model to simulated diffuse light flashes are represented as space-time plots. The firing pattern of each cell in the model is represented as a row of dots; each dot represents the time of occurrence of an action potential in that cell. Firing patterns of subpial cells are represented at the top of the figure, followed by those of horizontal cells, stellate cells, medial pyramidal cells and lateral pyramidal cells. Individual cells within each group are ordered by their approximate positions along the rostral-caudal axis of the model, so that their firing latencies are an index of the progression of the wave across the cortex. (A) Response of the model with all synaptic interactions intact. (B) Response of the model with the synapses of subpial cells on other neurons blocked.

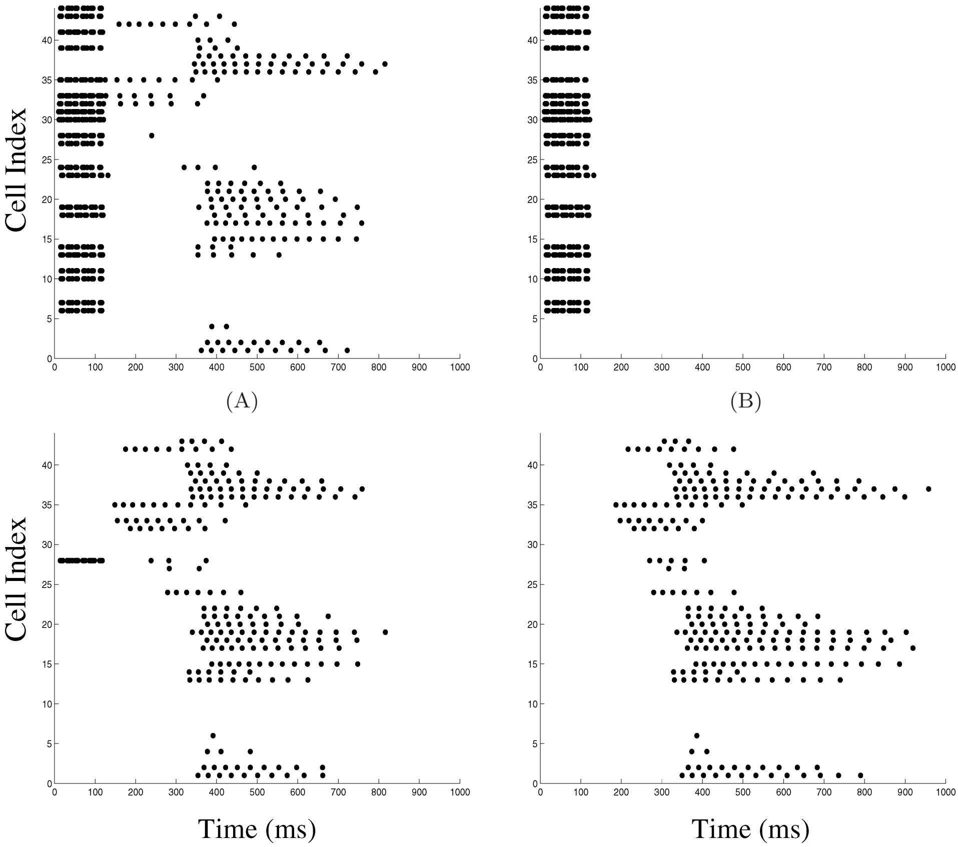

(A) (B)

(C) (D)

Fig. 10. Firing patterns of subpial cells. This figure shows the firing patterns of the 44 subpial cells in the large-scale model. The vertical axis in each plot is an index of the individual subpial cells. The horizontal axis represents time after stimulus presentation. Thus, the bottom horizontal line of dots shows the firing times of subpial cell 1; the top horizontal line of dots shows the firing times of subpial cell 44. (A) Responses of the 44 subpial cells to a diffused light flash, simulated by simultaneously activating all 201 geniculate neurons for 150 ms. (B) Responses of the 44 subpial cells with all recurrent excitation from pyramidal cell collaterals blocked. (C) Responses of the 44 subpial cells to simultaneous activation of geniculate neurons 1–20 and 61–80. (D) Responses of the 44 subpial cells to simultaneous activation of geniculate neurons 1–20 and 21–40.

[illegible] (F [illegible] 10B). [illegible]

[illegible] 150 [illegible] F [illegible] 10C [illegible]

[illegible] 1 20 [illegible] 61 80. [illegible] 28 [illegible] 220 [illegible] 400 [illegible] 71 [illegible] 74. [illegible] F [illegible] 10D [illegible] 1 20 [illegible] 21 40. [illegible] C [illegible]

3.3. *Responses of subpial cells to simulated apparent motion stimuli*

[illegible] 21 [illegible] 60 [illegible] 125 [illegible] ([illegible] 82 106 [illegible] 108 132) [illegible] (F [illegible] 11). F [illegible] 11A [illegible] F [illegible] 11B [illegible] 11C [illegible] 100 [illegible] 120 [illegible]

3.4. *Responses of subpial cells to simulated moving stimuli*

F [illegible] 12 [illegible] ([illegible]) [illegible] 150 [illegible] 6 [illegible] 120 [illegible] F [illegible] 12A [illegible] 12B [illegible]

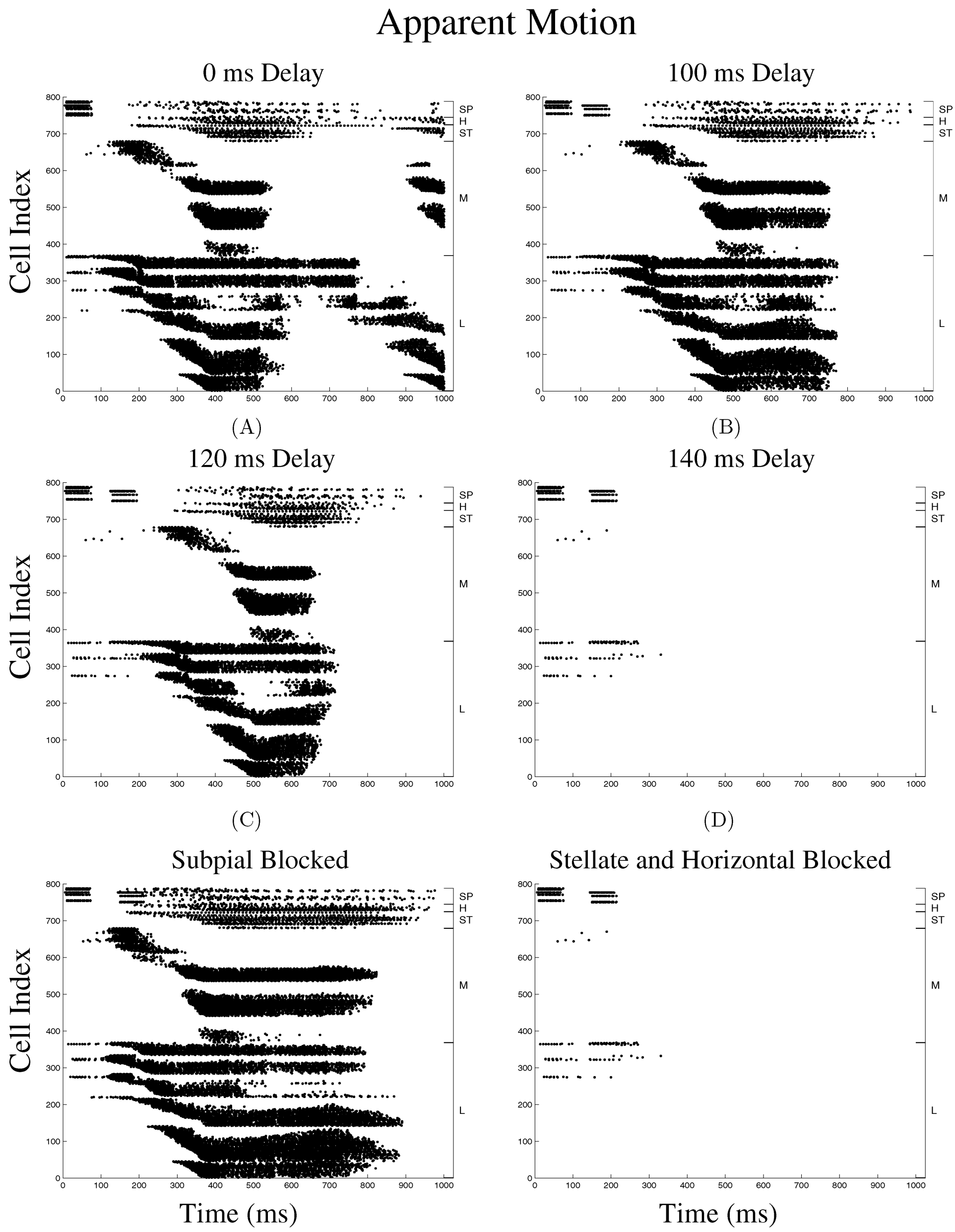

(A) (B)

(C) (D)

(F) (F)

Fig. 11. Responses of subpial cells to simulated apparent motion stimuli. Response of the large scale model to activation of two groups of 25 geniculate neurons each with a range of delays between the onset of the first and second groups. The first group consisted of neurons 82–106; the second group consisted of neurons 108–132. (A) Simultaneous activation of the two groups of neurons (that is, a delay of 0 ms). (B) Activation of the two groups of neurons with a delay of 100 ms. (C) Activation of the two groups of neurons with a delay of 120 ms. (D) Activation of the two groups of neurons with a delay of 140 ms. (E) Activation of the two groups of neurons with a delay of 140 ms and the inhibition from subpial cells to other cells in the cortex blocked. (F) Activation of the two groups of neurons with a delay of 140 ms and the inhibition from stellate and horizontal cells to other cells in the cortex blocked.

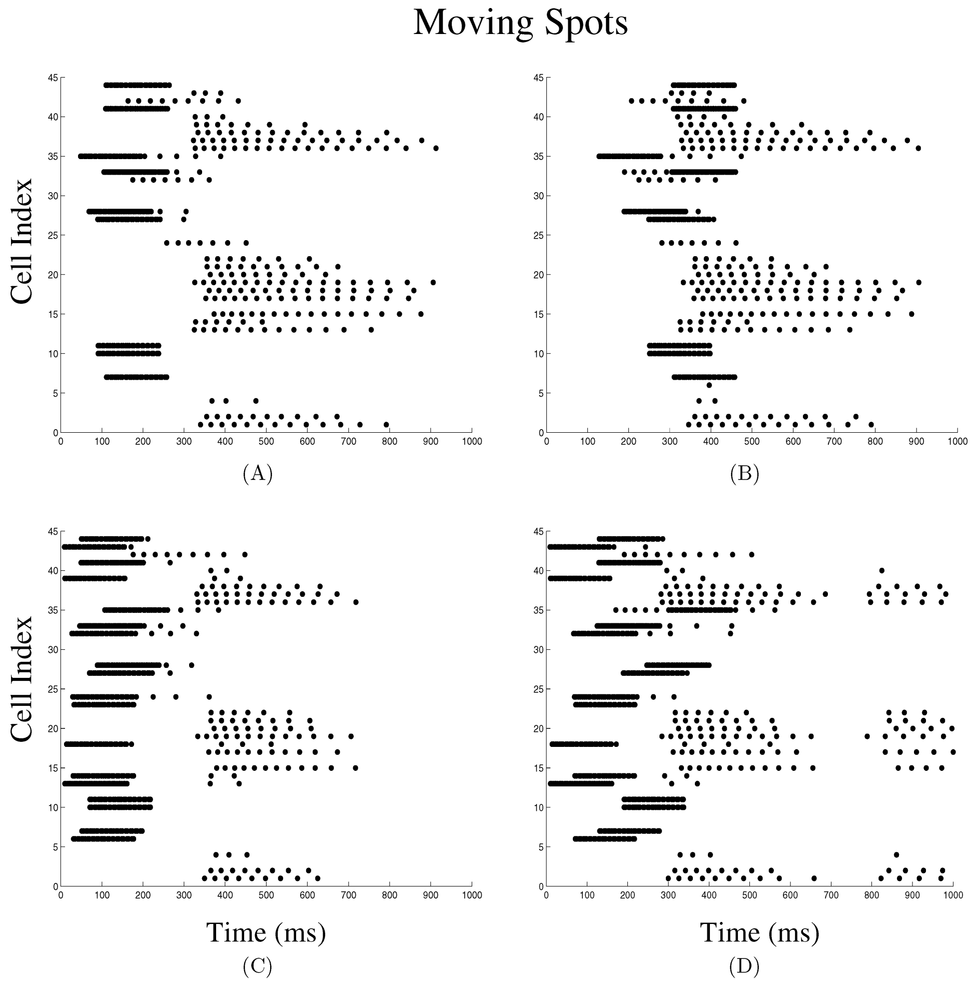

(A) (B)

(C) (D)

Fig. 12. Responses of subpial cells to simulated moving stimuli. Responses of the subpial cells in the large scale model to four different stimuli moving either from left to right or from right to left with delays of 20 ms and 60 ms, respectively. The 6 groups of geniculate neurons in the case of stimuli moving from left to right were neurons 1–20, 21–40, 41–60, 61–80, 81–100 and 101–120 along the row of geniculate neurons. The 6 groups of geniculate neurons in the case of stimuli moving from right to left were neurons 141–160, 121–140, 101–120, 81–100, 61–80 and 41–60. Each space-time plot shows the firing pattern of all of the subpial cells to sequential activation of a sequence of geniculate neurons. (A) Responses of the subpial cells to a stimulus moving from left to right with delays of 20 ms. (B) Responses of the subpial cells to a stimulus moving from left to right with delays of 60 ms. (C) Responses of the subpial cells to a stimulus moving from right to left with delays of 20 ms. (D) Responses of the subpial cells to a stimulus moving from right to left with delays of 60 ms.

[illegible] 20 [illegible] 60 [illegible]

1 20, 21 40, 41 60, 61 80, 81 100 [illegible] 101 120 [illegible]

F [illegible] 12C [illegible] 12D [illegible]

[illegible] 20 [illegible] 60 [illegible]

141 160, 121 140, 101 120, 81 100, 61 80 41 60. A H- F 12A 12B F 12C 12D 26

3.5. *Effects of subpial cell inhibition on pyramidal cells*

(F 9A) *et al.* 37. A 20 150 37 150 450 600 600 800 A F 9A 150 F 9B.

F 11B 11C . F 11D 140 A

[illegible] F[illegible] 11E [illegible] 11F [illegible] F[illegible] 11D. H[illegible] (F[illegible] 11E) [illegible] (F[illegible] 11F) [illegible]. A [illegible]

4. Discussion

4.1. *Are superficial units the same as subpial cells?*

A [illegible] 21 [illegible] D[illegible] 9 [illegible] C[illegible] *et al.* 6. [illegible] H[illegible] *in vivo* [illegible] *in vitro* [illegible] *et al.* 9), [illegible] 6 [illegible].

4.2. *Limitations of the detailed model of subpial cells and the large-scale model of the cortex*

[illegible] 3-12-99 [illegible] C[illegible] *et al.* 6. [illegible] 12 [illegible] 3-12-99 [illegible]

[illegible]. H [illegible] [23, 30].

4.3. *Subpial cells have wide receptive fields*

[illegible] [21] [illegible]. H [illegible] 10% [illegible] 30% [illegible] [6]. [illegible] [36]. G [illegible] *en passant* [22]. E [illegible]. C [illegible]. A [illegible]

[illegible]. H [illegible] 10° [illegible] 40° [illegible] [4, 21]. C [illegible] 40°. C [illegible] 1° [illegible] 60°. C [illegible].

[illegible] *in vivo* [illegible].

4.4. *Subpial cells fire in two phases*

[illegible] 21 [illegible] A [illegible] A [illegible] H [illegible] A [illegible] 150 [illegible] 15, 19 [illegible].

4.5. *Subpial cell activation leads the activation of pyramidal cells*

[illegible] 21 [illegible] 2. [illegible]

[illegible] B [illegible] *in vitro* [illegible] ([illegible] *et al.* 21). E [illegible] 2 [illegible] 157.8 [illegible] 220.8 [illegible] 21. [illegible] 639 ± 64 [illegible] B [illegible], [illegible] E [illegible] 109.0 [illegible] 137.3 [illegible] 280 ± 35 [illegible]

[illegible] (C [illegible], [illegible]) [illegible] 13,000 [illegible] A [illegible] 14, [illegible] 26 [illegible] 92% [illegible] A [illegible] 13,000 [illegible] 2000 μ [illegible], [illegible] 210 μ [illegible] 1400 [illegible] *et al.* 32 [illegible] 1800 [illegible], [illegible] 100 μ [illegible] ([illegible]., [illegible]) [illegible]

[illegible] 12, 38, [illegible] 1400 [illegible]. [illegible] 138 [illegible]. [illegible], [illegible], [illegible]. C [illegible] *et al.* 19 [illegible] 100 [illegible] /μ / [illegible]

A [illegible]. [illegible]

(723 ± 109 131 ± 14)
(45.5 ± 5.2 140 ± 62) 6, 8, 19.
1.1 ± 0.2 6 E
25%
E

A

A

B

H

D
D
(1, 11, 18).
(1, 25).

4.6. *Function of subpial cells*

BJ

[illegible]

Acknowledgments

[illegible] C [illegible] C [illegible] F [illegible] B. . G [illegible] . [illegible] F [illegible] C [illegible].

References

1. A[illegible] G[illegible] C[illegible], [illegible] G, [illegible] C [illegible] DA, [illegible], *Cereb Cortex* **7**:1047 3211, 1997.
2. B[illegible] G, [illegible] A[illegible] [illegible], *J Neurophys* **67**:1185 1200, 1992.
3. B[illegible] G, [illegible] A[illegible] E [illegible] γ- [illegible], *J Comp Neurol* **259**:277 297, 1987.
4. B[illegible], [illegible], *Emys orbicularis, Neurosci Behav Physiol* **10**:183 188, 1980.
5. B[illegible], B[illegible] D, *The Book of Genesis*, 2 [illegible]., E[illegible], 1998.
6. C[illegible] B, [illegible], B[illegible] [illegible], *J Comp Neurol* **471**:333 351, 2004.
7. C[illegible] B, [illegible], *J Comput Neurosci* **7**:71 87, 1999.
8. C[illegible] B, [illegible] A[illegible] [illegible] D[illegible], *J Neurosci* **6**:164 177, 1986.
9. D[illegible] H, [illegible], *Pseudemys scripta elegans.* .D. [illegible] H [illegible] C [illegible] A, 1984.
10. D[illegible], G [illegible] B [illegible] E [illegible], *IEEE Trans Biomed Eng* **52**:566 577, 2005.
11. F[illegible] F, [illegible] AC, [illegible] AD, [illegible], G[illegible] [illegible] G [illegible], *J Comp Neurol* **221**:263 278, 1983.
12. H[illegible] A, F[illegible] E, E[illegible] FF, H[illegible] C, [illegible] (*Pseudemys scripta* [illegible] *Chrysemys picta*), *Brain Res* **130**:197 216, 1997.
13. H[illegible] B, [illegible] *Pseudemys* [illegible] *Chrysemys*, *Anat Embryol* **175**:505 515, 1987.
14. [illegible] B, [illegible] - , B[illegible] G, [illegible], H[illegible], C[illegible] DD, [illegible] E , F[illegible], *Emys orbicularis.* A G[illegible] H[illegible] GABA [illegible], *J Comp Neurol* **356**:595 614, 1995.
15. [illegible] A[illegible] [illegible], *J Neurosci* **7**:2488 2492, 1987.
16. [illegible] A[illegible] C[illegible] B[illegible] [illegible], *J Neurosci* **6**:178 191, 1986.

17 [illegible], E[illegible] [illegible], *J Neurophysiol* **66**:293–306, 1991.

18 [illegible] 17, [illegible] (*Macaca mulatta*), *J Comp Neurol* **147**:455–496, 1973.

19 [illegible] G, F[illegible] *Vis Neurosci* **15**:979–993, 1998.

20 [illegible] G, [illegible] GABA$_A$- [illegible], *Vis Neurosci* **18**:9–24, 2001.

21 [illegible] *Emys orbicularis*, *J Evol Biochem Physiol* **8**:550–555, 1972.

22 [illegible] A, [illegible], *J Comp Neurol* **296**:531–547, 1990.

23 [illegible] I, G [illegible] B, [illegible], *IEEE Trans Biomed Eng* **49**:753–762, 2002.

24 [illegible] I, G [illegible] B, [illegible] A [illegible], *J Comput Neurosci* **14**:161–184, 2003.

25 [illegible] H, H[illegible] D[illegible], [illegible] A[illegible], [illegible] CA1 [illegible], *J Comp Neurol* **443**:346–367, 2002.

26 [illegible] *Pseudemys* [illegible] *Chrysemys*, *J Comp Neurol* **253**:440–465, 1986.

27 [illegible], [illegible] *Biophys J* **9**:1483–1508, 1969.

28 [illegible] A, A [illegible], *Brain Behav Evol* **38**:53–91, 1991.

29 [illegible] A, [illegible] D[illegible], E[illegible], *J Comput Neurosci* **16**:267–298, 2004.

30 [illegible] D, [illegible] *Vis Neurosci* **16**:65–79, 1999.

31 [illegible] D, [illegible] A, H[illegible] D [illegible] *J Neurophysiol* **87**:1499–1514, 2002.

32 [illegible], E[illegible] FF, C [illegible] *Pseudemys* [illegible]: A [illegible], *J Comp Neurol* **190**:445–461, 1980.

33 [illegible], [illegible] A, [illegible] A, [illegible] G, [illegible] B, [illegible] D[illegible] C, [illegible] G ([illegible]), *The Computing Neuron*, A[illegible], 296–321, 1989.

34 [illegible], *Pseudmys scripta*, *J Comp Neurol* **254**:529–542, 1986.

35 [illegible] EG, [illegible] A ([illegible]), *Cerebral Cortex, Vol. 13. Models of Cortical Circuitry*, [illegible] 283–399, 1999.

36. [illegible], [illegible] *Pseudemys* [illegible] *Chrysemys*, *J Comp Neurol* **276**:92 112, 1988.

37. [illegible], C [illegible] C, G [illegible] B, [illegible], *J Comput Neurosci* **19**:263 289, 2005.

38. [illegible] D, [illegible] H, B [illegible], [illegible], [illegible] *Pseudemys scripta elegans*, *Brain Behav Evol* **65**:278 292, 2005.